Electronic Supplementary Material (ESI) for Integrative Biology

Supplemental Materials for "Differential parsing of EGFR endocytic flux among parallel internalization pathways in lung cancer cells with EGFR-activating mutations,"
Alice M. Walsh and Matthew J. Lazzara

Supplemental Materials and Methods:

Cell lysis and western blotting. Whole cell lysates were prepared in a standard cell extraction buffer (Life Technologies) supplemented with protease and phosphatase inhibitors (Sigma). Lysates were cleared by centrifugation at 13,200 rpm for 10 min, and total protein concentrations were determined by micro-bicinchoninic assay (Thermo Scientific). Approximately 20 µg of total protein was loaded per lane on 4-12% gradient polyacrylamide gels (Life Technologies) under denaturing and reducing conditions and transferred to 0.2 µm nitrocellulose membranes (Life Technologies). After probing with antibodies, membranes were imaged on a LI-COR Odyssey scanner (LI-COR). Membranes were stripped with 0.2 M NaOH as needed.

Estimation of number of EGFR per cell. Recombinant human EGF (Peprotech) was labeled with ^{125}I as described previously.[1] Cells were starved overnight in media containing 0.1% FBS (Life Technologies) and then treated with 10 ng/mL ^{125}I-EGF on ice for 30 min. After washing with buffer to remove un-bound ^{125}I-EGF, the amount of cell surface-associated radioactivity was quantified by stripping surface-bound ligand from receptors using a mild acid strip. These samples were used to calculate the number of EGFR per cell based on the known EGF/EGFR dissociation constant and the specific activity of the labeled EGF. Three plates were reserved to determine the number of cells per plate by counting with a hemocytometer.

Supplemental Figures:

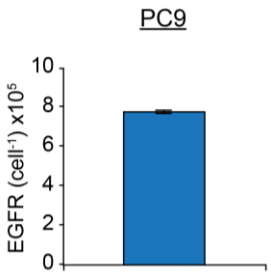

Supplemental Figure 1. Measurement of number of EGFR per cell in PC9 cells. The number of EGFR per cell in PC9 cells was calculated using ^{125}I-EGF binding as described in *Supplemental Materials and Methods*. Data represents the mean of three replicates ± s.d.

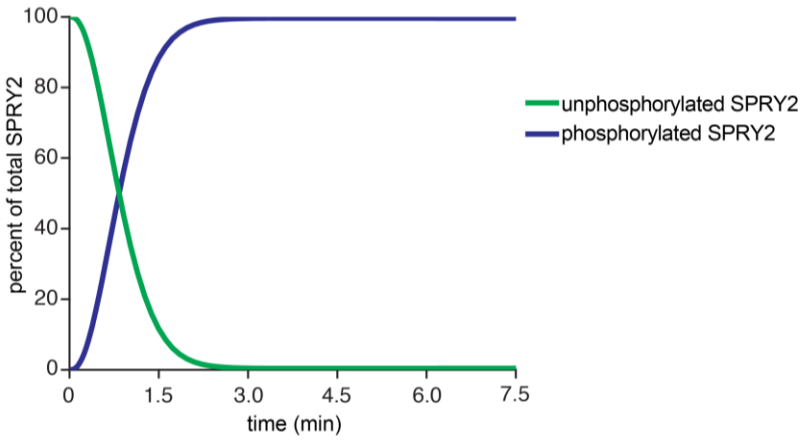

Supplemental Figure 2. Simulation of SPRY2 phosphorylation. SPRY2 phosphorylation with 10 ng/mL EGF treatment was simulated over the time course of an EGFR k_e measurement. Base model conditions with standard parameters for H1666 cells were used. SPRY2 phosphorylation parameters were estimated to agree with data from Mason et al.[2] such that peak SPRY2 phosphorylation occurred by 3 min after EGF addition.

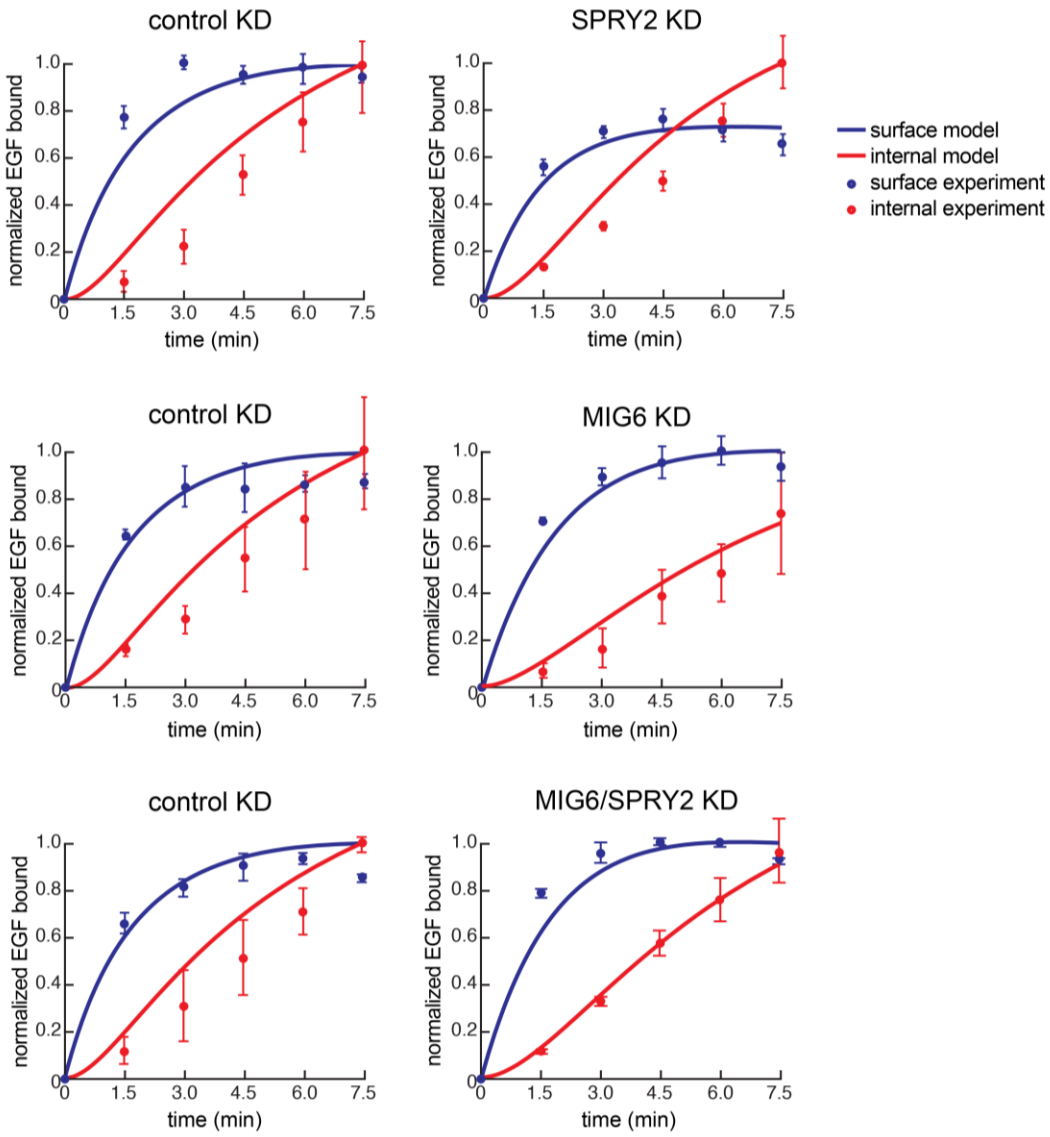

Supplemental Figure 3. Predicted and experimental measurements of internal and surface-bound EGF for H1666 cells. The k_i parameters were fit to k_e data from H1666 cells as described in Fig. 2A. Shown here are the primary experimental data from the study by Walsh and Lazzara[1] used to experimentally determine k_e values and the ability of the model to recapitulate the dynamics of surface and internal ^{125}I-EGF. Markers represent the mean of three experimental replicates ± s.d.

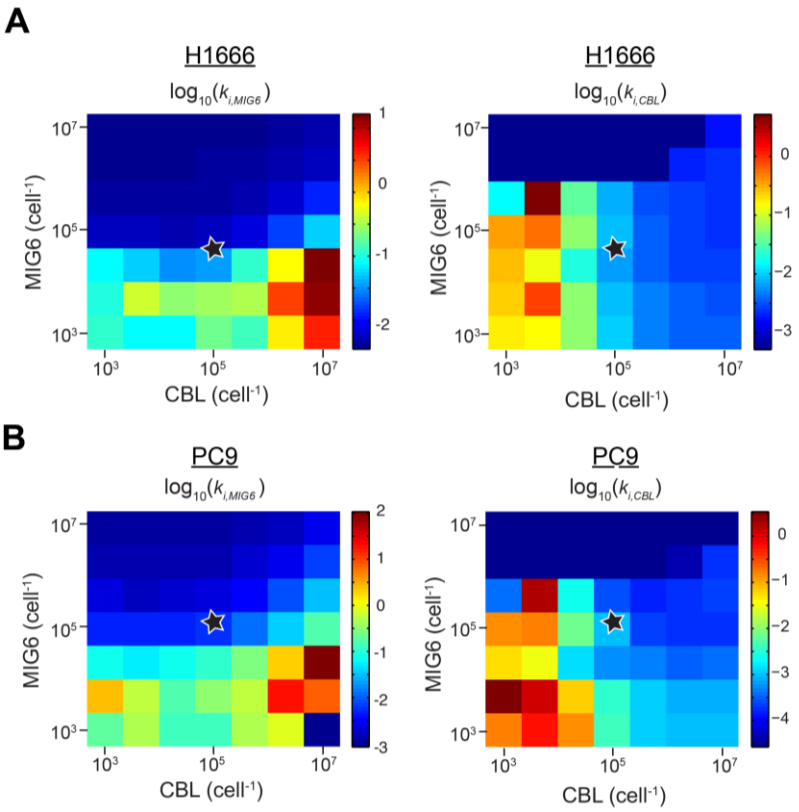

Supplemental Figure 4. Values of fitted rate constants for a range of MIG6 and CBL concentrations. The k_i parameters were fit to data from (*A*) H1666 cells or (*B*) PC9 cells as described in Figs. 2C and Fig. 3C. Stars indicate the base MIG6 and CBL concentrations ([MIG6] = 5×10^4 cell^{-1} (H1666) or 1.2×10^5 cell^{-1} (PC9) and [CBL] = 1×10^5 cell^{-1}).

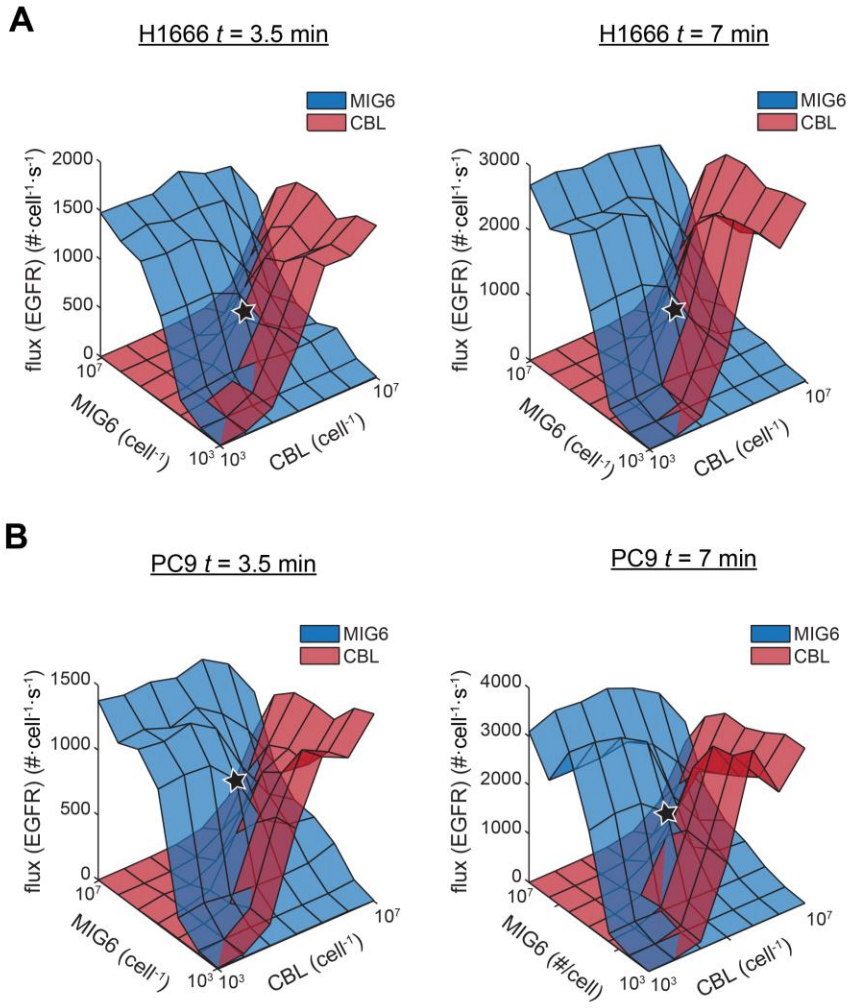

Supplemental Figure 5. EGFR internalization flux over a range of MIG6 and CBL concentrations. EGFR flux is plotted for receptors internalized by MIG6 or CBL pathways at t = 3.5 min or 7 min for (*A*) H1666 cells and (*B*) PC9 cells. Stars indicate the base MIG6 and CBL concentrations ([MIG6] = 5×10^4 cell^{-1} (H1666) or 1.2×10^5 cell^{-1} (PC9) and [CBL] = 1×10^5 cell^{-1}).

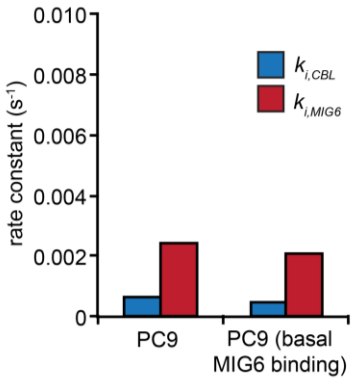

Supplemental Figure 6. Effect of allowing basal MIG6/EGFR association on model fit to PC9 data. The k_i parameters were fit to data from PC9 cells as in Fig. 3 and then by allowing basal MIG6/EGFR association for non-ligand-bound EGFR dimers using standard MIG6 and CBL concentrations.

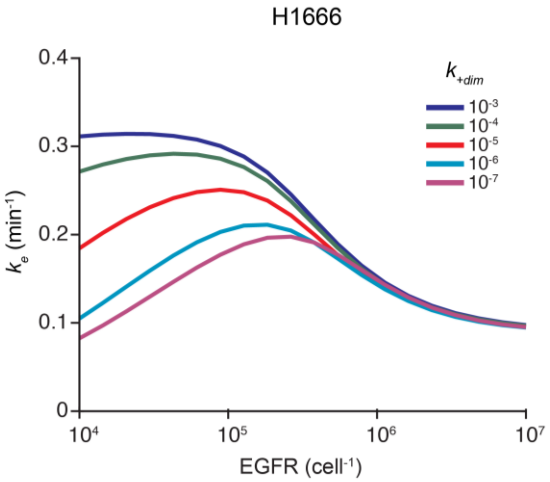

Supplemental Figure 7. Predicted effect of changing dimerization rate on relationship between EGFR expression and predicted EGFR k_e. For parameters fit to data from H1666 cells, k_{+dim} was set to values between 10^{-3} and 10^{-7} cell s^{-1}, and the predicted k_e was calculated for a range of EGFR concentrations as in Fig. 4A. This demonstrates that the increase in k_e with increasing EGFR expression arises due to an increased driving force for EGFR dimerization.

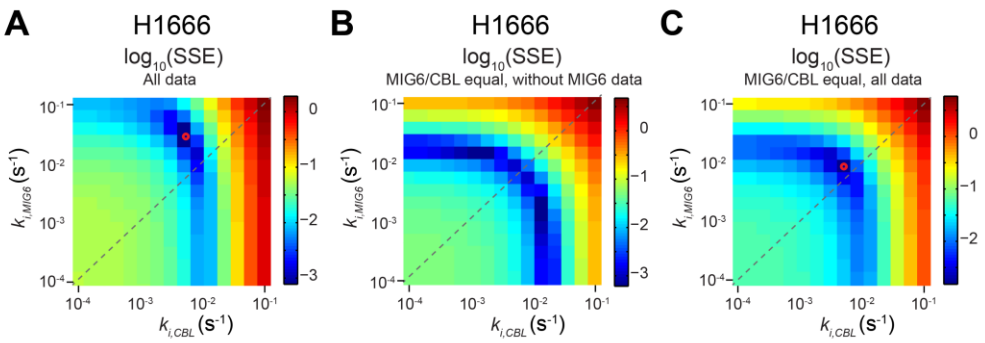

Supplemental Figure 8. Model agreement with H1666 data. Model error was calculated considering: (*A*) all data points with normal model conditions, (*B*) data excluding MIG6 knockdown data with [MIG6] = [CBL] = 1×10^5 cell^{-1}, $k_{on,M} = k_{on,C}$, and $k_{on,S} = 0$, and (*C*) the same conditions for *C* including all data. The log of the sum of the squares error (SSE) is plotted for a range of $k_{i,MIG6}$ and $k_{i,CBL}$. Error minima are indicated by red circles. The dashed lines represent $k_{i,MIG6} = k_{i,CBL}$.

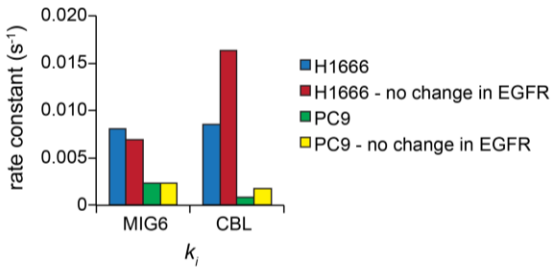

Supplemental Figure 9. Fitted parameters when changes in EGFR expression due to SPRY2 knockdown are not considered. The k_i parameters were fit to experimental EGFR k_e data for controls, MIG6 knockdown, and SPRY2 knockdown from H1666 or PC9 cells using standard MIG6 and CBL concentrations as described for Figs. 2 and 3. The k_i parameters were also fit without changing EGFR concentration for SPRY2 knockdown conditions.

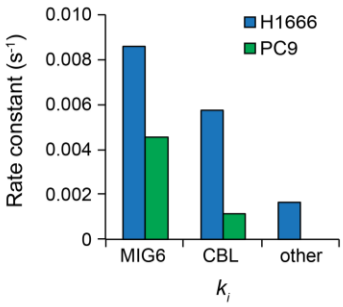

Supplemental Figure 10. Values of fitted rate constants when f_r was set to experimentally determined values. The k_i parameters were fit to all data points from H1666 or PC9 cells using standard MIG6 and CBL concentrations ([MIG6] = 5×10^4 cell^{-1} (H1666) or 1.2×10^5 cell^{-1} (PC9) and [CBL] = 1×10^5 cell^{-1}) and setting f_r to experimentally determined values.

Supplemental Table 1. Model equations for individual species.

Species Number	Model Species	ODE	Description
1	R	R1 -R2 -2*R3 -R5 -R28 -keb*R	EGFR monomer
2	RL	R2 -R5 -2*R7 -R29 -keb*RL	EGFR monomer + ligand
3	D	R3 -R4 -R30 -keb*D	EGFR dimer
4	DL	R4 +R5 -R6 -R18 -R31 -R57 -keb*DL	Dimer + ligand
5	DLL	R6 +R7 -R23 -R32 -R58 -keb*DLL	Dimer + 2 ligands
6	M	-R18 -R23 +R51 +R53	MIG6
7	DLM	R18 -R22 -R37 -keb*DLM	Dimer + ligand + MIG6
8	DLLM	R22 +R23 -R39 -keb*DLLM	Dimer + 2 ligands + MIG6
9	Ri	R28 -R41 +keb*R	Internalized EGFR
10	RLi	R29 -R43 +keb*RL	Internalized EGFR + ligand
11	Di	R30 -R44 +keb*D	Internalized dimer
12	DLi	R31 -R45 +keb*DL	Internalized dimer + ligand
13	DLLi	R32 -R46 +keb*DLL	Internalized dimer + 2 ligands
14	DLMi	R37 -R51 +keb*DLM	Internalized dimer + ligand + MIG6
15	DLLMi	R39 -R53 +keb*DLLM	Internalized dimer + 2 ligands + MIG6
16	C	-R57 -R58 +R61 +R62 -R63	CBL
17	DLC	R57 -R56 -R59 -keb*DLC	Dimer + ligand + CBL
18	DLLC	R58 +R56 -R60 -keb*DLLC	dimer + 2 ligands + CBL
19	DLCi	R59 -R61 +keb*DLC	Internalized dimer + ligand + CBL
20	DLLCi	R60 -R62 +keb*DLLC	Internalized dimer + 2 ligands + CBL
21	Sp	-R63 -R70 +R69	Phosphorylated SPRY2
22	CSp	R63	CBL + phosphorylated SPRY2
23	kin	-R68 +R69	SPRY2 kinase
24	S	-R68 +R70	SPRY2
25	kinS	R68 -R69	SPRY2 kinase + SPRY2

Supplemental Table 2. Model reactions included in the ODEs in Supplemental Table 1.

Reaction Name	Reaction Equation	Description
R1	s1	EGFR synthesis
R2	f2*R*L - r2*RL	EGF binding
R3	f3*R*R - r3*D	EGF binding
R4	2*f4*D*L - r4*DL	Dimerization
R5	f5*R*RL - r5*DL	Dimerization
R6	f6*DL*L - 2*r6*DLL	EGF binding
R7	f7*RL*RL - r7*DLL	Dimerization
R18	2*f18*DL*M - r18*DLM	MIG6 binding
R22	f22*DLM*L - 2*r22*DLLM	EGF binding
R23	2*f23*DLL*M - r23*DLLM	MIG6 binding
R28	k28*R - kr*Ri*fru	Internalization/recycling
R29	k29*RL - kr*RLi*fr	Internalization/recycling
R30	k30*D- kr*Di*fru	Internalization/recycling
R31	k31*DL - kr*DLi*fr	Internalization/recycling
R32	k32*DLL - kr*DLLi*fr	Internalization/recycling
R37	k37*DLM - kr*DLMi*fr	Internalization/recycling
R39	k39*DLLM - kr*DLLMi*fr	Internalization/recycling
R41	kd*Ri*(fdu)	Degradation
R43	kd*RLi*(fd)	Degradation
R44	kd*Di*(fdu)	Degradation
R45	kd*DLi*(fd)	Degradation
R46	kd*DLLi*(fd)	Degradation
R51	kd*DLMi*(fd)	Degradation
R53	kd*DLLMi*(fd)	Degradation
R56	f56*DLC*L - 2*r56*DLLC	EGF binding
R57	2*f57*DL*C - r57*DLC	CBL binding
R58	2*f58*DLL*C - r58*DLLC	CBL binding
R59	k59*DLC - kr*DLCi*fr	Internalization/recycling
R60	k60*DLLC - kr*DLLCi*fr	Internalization/recycling
R61	kd*DLCi*(fd)	Degradation
R62	kd*DLLCi*(fd)	Degradation
R63	f63*C*Sp - r63*CSp	CBL binding
R68	f68*S*kin*(Ligand-bound EGFR dimers/total EGFR) - r68*kinS;	SPRY2/kinase binding
R69	f69*kinS	SPRY2 phosphorylation
R70	r70*Sp	SPRY2 dephosphorylation

Supplemental Table 3. Parameters for model equations.

Parameter	Description	Typical Value
s1	EGFR synthesis	$0\ s^{-1}$
f2, f4	$k_{on,L}$	$1\times10^{6}\ M^{-1}s^{-1}$
f3, f5	k_{+dim}	2.6×10^{-8} cell s^{-1}
f6, f22, f56	$k_{on,L2}$	$1\times10^{5}\ M^{-1}s^{-1}$
f7	k_{+dim2}	2.6×10^{-5} cell s^{-1}
f18, f23	$k_{on,M}$	2×10^{-5} cell s^{-1}
r2, r4, r6, r22, r56	$k_{off,L}$	$2.7\times10^{-3}\ s^{-1}$
r3, r5, r7	k_{-dim}	$1\times10^{-1}\ s^{-1}$
r18, r23	$k_{off,M}$	$1\ s^{-1}$
keb	$k_{i,basal}$	$3.8\times10^{-4}\ s^{-1}$
k28	R internalization	0
k29	RL internalization	0
k30	D internalization	0
k31, k32	Other internalization	$k_{i,other}$ (fitted)
k37, k39	MIG6 internalization	$k_{i,MIG6}$ (fitted)
k59, k60	CBL internalization	$k_{i,CBL}$ (fitted)
kd	k_{deg}	$6\times10^{-4}\ s^{-1}$
kr	k_{rec}	$3.4\times10^{-3}\ s^{-1}$
fr	f_r	0.5
fru	$f_{r,\ unbound}$	1
f57, f58	$k_{on,C}$	4×10^{-6} cell s^{-1}
r57, r58	$k_{off,C}$	$1\ s^{-1}$
f63	$k_{on,S}$	1×10^{-5} cell s^{-1}
r63	$k_{off,S}$	$1\times10^{-1}\ s^{-1}$
f68	SPRY2/kinase k_{on}	1×10^{-5} cell s^{-1}
r68	SPRY2/kinase k_{off}	$1\times10^{-1}\ s^{-1}$
f69	SPRY2 phosphorylation k_{cat}	$1\times10^{-1}\ s^{-1}$
r70	SPRY2 dephosphorylation	$1\times10^{-3}\ s^{-1}$

Supplemental Table 4. Parameter values based on literature.

Parameter	Value	Reference
$k_{on,L}$ [$M^{-1}s^{-1}$]	1×10^{6}	Berkers 1991, Felder 1992, French 1995 [3-5]
$k_{off,L}$ [s^{-1}]	2.7×10^{-3}	Berkers 1991, Felder 1992, French 1995 [3-5]
$k_{on,L2}$ [$M^{-1}s^{-1}$]	1×10^{5}	Berkers 1991, Felder 1992, Macdonald-Obermann 2009 [3, 4, 6]
k_{+dim} [cell s^{-1}]	2.6×10^{-8}	Macdonald-Obermann 2009 [4]
k_{+dim2} [cell s^{-1}]	2.6×10^{-5}	Kholodenko 1999, Schoeberl 2009, Monast 2012 [7-9]
k_{-dim} [s^{-1}]	1×10^{-1}	Kholodenko 1999, Schoeberl 2009 [8, 9]
k_{deg} [s^{-1}]	6×10^{-4}	Hendriks 2003, Hendriks 2006, Schoeberl 2009 [9-11]
k_{rec} [s^{-1}]	3.4×10^{-3}	Hendriks 2003, Hendriks 2006, Schoeberl 2009 [9-11]
Cell volume [L]	5.2×10^{-13}	Calculated
H1666 f_r	0.574	Walsh 2013 [1]
PC9 f_r	0.899	Walsh 2013 [1]

Supplemental Table 5. Estimated parameter values and initial model species concentrations.

Parameter	H1666	PC9	Reference
MIG6 [$cell^{-1}$]	1.2×10^{5}	5×10^{4}	Estimated and western blotting [1]
SPRY2 [$cell^{-1}$]	5×10^{4}	5×10^{4}	Estimated and western blotting [1]
CBL [$cell^{-1}$]	1×10^{5}	1×10^{5}	Estimated
EGFR [$cell^{-1}$]	6×10^{5}	8×10^{5}	Based on ^{125}I-EGF binding and western blotting [1]
EGFR (SPRY2 KD) [$cell^{-1}$]	3.6×10^{5}	4×10^{5}	Walsh 2013 [1]
EGFR (SPRY2 KD+EGFR) [$cell^{-1}$]	1.2×10^{6}	8×10^{5}	Walsh 2013 [1]
SPRY2 kinase [$cell^{-1}$]	1×10^{5}	1×10^{5}	Estimated
$k_{i,basal}$ [s^{-1}]	3.8×10^{-4}	3.8×10^{-4}	fitted
$k_{on,C}$ [cell s^{-1}]	4×10^{-6}	4×10^{-6}	Hsieh 2010, Ng 2008, Nguyen 2000 [12-14]
$k_{off,C}$ [s^{-1}]	1	1	Hsieh 2010, Ng 2008, Nguyen 2000 [12-14]
$k_{on,M}$ [cell s^{-1}]	2×10^{-5}	2×10^{-5}	Zhang 2007 [15]
$k_{off,M}$ [s^{-1}]	1	1	Zhang 2007 [15]
$k_{on,S}$ [cell s^{-1}]	1×10^{-5}	1×10^{-5}	Ng 2008 [12]
$k_{off,S}$ [s^{-1}]	1×10^{-1}	1×10^{-1}	Ng 2008 [12]
SPRY2/kinase binding	$k_{on} = 1\times10^{-5}$ cell s^{-1}; $k_{off} = 1\times10^{-1}$ s^{-1}	$k_{on} = 1\times10^{-5}$ cell s^{-1}; $k_{off} = 1\times10^{-1}$ s^{-1}	Northrup 1992, Kholodenko 1999, [8, 16]
SPRY2 phosphorylation k_{cat} [s^{-1}]	1×10^{-1}	1×10^{-1}	Estimated based on Mason 2004 [2]
SPRY2 dephosphorylation [s^{-1}]	1×10^{-3}	1×10^{-3}	Estimated based on Mason 2004 [2]

Supplemental Table 6. Normalized experimental k_e data.

Measurement	H1666	PC9
k_e (min^{-1}) control	0.170	0.058
k_e (min^{-1}) MIG6 KD	0.116	0.034
k_e (min^{-1}) SPRY2 KD	0.219	0.091
k_e (min^{-1}) MIG6/SPRY2 KD	0.149	0.038
k_e (min^{-1}) SPRY2 KD + EGFR	0.148	0.058

Supplemental Table 7. Full results of local parameter sensitivity analysis.

H1666 parameter	|Normalized sensitivity|	PC9 parameter	|Normalized sensitivity|
$k_{off,kinS}$	4.65×10^{-5}	$k_{i,other}$	4.41×10^{-7}
k_{dephos}	0.00117	k_{dephos}	1.96×10^{-5}
$k_{on,kinS}$	0.00132	$k_{cat,S}$	5.65×10^{-5}
$k_{cat,S}$	0.00180	$k_{off,kinS}$	8.73×10^{-5}
$k_{on,L2}$	0.00237	$k_{on,kinS}$	0.000451
$f_{r,unbound}$	0.00363	$k_{on,S}$	0.000481
$k_{off,L}$	0.00720	$k_{off,S}$	0.000500
k_{+dim2}	0.00987	$k_{on,C}$	0.00192
k_{+dim}	0.0187	$k_{off,C}$	0.00222
$k_{on,S}$	0.0226	$k_{on,L2}$	0.00340
$k_{off,S}$	0.0254	k_{+dim}	0.00467
k_{-dim}	0.0270	$f_{r,unbound}$	0.00513
k_{deg}	0.0384	k_{-dim}	0.00620
$k_{off,M}$	0.0600	$k_{off,L}$	0.00665
$k_{on,M}$	0.0602	k_{+dim2}	0.00755
$k_{i,basal}$	0.110	k_{deg}	0.0414
$k_{off,C}$	0.127	$k_{i,CBL}$	0.0505
$k_{on,C}$	0.1303	$k_{on,M}$	0.138
$k_{i,other}$	0.198	$k_{off,M}$	0.139
f_r	0.207	f_r	0.208
k_{rec}	0.247	k_{rec}	0.252
$k_{i,CBL}$	0.273	$k_{i,basal}$	0.265
$k_{on,L}$	0.284	$k_{on,L}$	0.290
$k_{i,MIG6}$	0.302	$k_{i,MIG6}$	0.629

References:

1. A. M. Walsh, M. J. Lazarra, Regulation of EGFR trafficking and cell signaling by Sprouty2 and MIG6 in lung cancer cells. *J Cell Sci* 2013, *126*. 4339-48 .

2. J. M. Mason, D. J. Morrison, B. Bassit, M. Dimri, H. Band, J. D. Licht, I. Gross, Tyrosine phosphorylation of Sprouty proteins regulates their ability to inhibit growth factor signaling: a dual feedback loop. *Mol Biol Cell* 2004, *15*. 2176-2188.

3. J. A. Berkers, P. M. van Bergen en Henegouwen, J. Boonstra, Three classes of epidermal growth factor receptors on HeLa cells. *J Biol Chem* 1991, *266*. 922-927.

4. S. Felder, J. LaVin, A. Ullrich, J. Schlessinger, Kinetics of binding, endocytosis, and recycling of EGF receptor mutants. *J Cell Biol* 1992, *117*. 203-212.

5. A. R. French, D. K. Tadaki, S. K. Niyogi, D. A. Lauffenburger, Intracellular trafficking of epidermal growth factor family ligands is directly influenced by the pH sensitivity of the receptor/ligand interaction. *J Biol Chem* 1995, *270*. 4334-4340.

6. J. L. Macdonald-Obermann, L. J. Pike, The intracellular juxtamembrane domain of the epidermal growth factor (EGF) receptor is responsible for the allosteric regulation of EGF binding. *J Biol Chem* 2009, *284*. 13570-13576.

7. C. S. Monast, C. M. Furcht, M. J. Lazzara, Computational analysis of the regulation of EGFR by protein tyrosine phosphatases. *Biophys J* 2012, *102*. 2012-2021.

8. B. N. Kholodenko, O. V. Demin, G. Moehren, J. B. Hoek, Quantification of short term signaling by the epidermal growth factor receptor. *J Biol Chem* 1999, *274*. 30169-30181.

9. B. Schoeberl, E. A. Pace, J. B. Fitzgerald, B. D. Harms, L. Xu, L. Nie, B. Linggi, A. Kalra, V. Paragas, R. Bukhalid, V. Grantcharova, N. Kohli, K. A. West, M. Leszczyniecka, M. J. Feldhaus, A. J. Kudla, U. B. Nielsen, Therapeutically targeting ErbB3: a key node in ligand-induced activation of the ErbB receptor-PI3K axis. *Sci Signal* 2009, *2*. ra31.

10. B. S. Hendriks, G. J. Griffiths, R. Benson, D. Kenyon, M. Lazzara, J. Swinton, S. Beck, M. Hickinson, J. M. Beusmans, D. Lauffenburger, D. de Graaf, Decreased internalisation of erbB1 mutants in lung cancer is linked with a mechanism conferring sensitivity to gefitinib. *Syst Biol (Stevenage)* 2006, *153*. 457-466.

11. B. S. Hendriks, H. S. Wiley, D. Lauffenburger, HER2-mediated effects on EGFR endosomal sorting: analysis of biophysical mechanisms. *Biophys J* 2003, *85*. 2732-2745.

12. C. Ng, R. A. Jackson, J. P. Buschdorf, Q. Sun, G. R. Guy, J. Sivaraman, Structural basis for a novel intrapeptidyl H-bond and reverse binding of c-Cbl-TKB domain substrates. *EMBO J* 2008, *27*. 804-816.

13. J. T. Nguyen, M. Porter, M. Amoui, W. T. Miller, R. N. Zuckermann, W. A. Lim, Improving SH3 domain ligand selectivity using a non-natural scaffold. *Chem Biol* 2000, *7*. 463-473.

14. M. Y. Hsieh, S. Yang, M. A. Raymond-Stinz, J. S. Edwards, B. S. Wilson, Spatio-temporal modeling of signaling protein recruitment to EGFR. *BMC Syst Biol* 2010, *4*. 57.

15. X. Zhang, K. A. Pickin, R. Bose, N. Jura, P. A. Cole, J. Kuriyan, Inhibition of the EGF receptor by binding of MIG6 to an activating kinase domain interface. *Nature* 2007, *450*. 741-744.

16. S. H. Northrup, H. P. Erickson, Kinetics of protein-protein association explained by Brownian dynamics computer simulation. *Proc Natl Acad Sci USA* 1992, *89*. 3338-3342.